27TH Conference on Hurricanes and Tropical Meteorology 24-28 April 2006, Monterey, CA

SENSTIVITY OF TROPICAL CYCLONE FORECASTS AS REVEALED BY SINGULAR VECTORS

Melinda S. Peng and Carolyn A. Reynolds
Marine Meteorology Division, Naval Research Laboratory
Monterey, CA

1. Introduction

Many efforts have been devoted to the understanding of tropical cyclones, their formation, evolutions and tracks. The primary quantities used to examine TC motion are vorticity in a barotropic environment (Chan et al. 2002) or potential vorticity (PV) in a baroclinic environment (Shapiro 1992). In this study, singular vector (SV) diagnostics are used to obtain information about the dynamical process that have an important impact on tropical cyclone evolution. Singular vector diagnostics have primarily been applied to mid-latitude phenomena (Reynolds et al. 2001). The SVs used in the present study are constructed to optimize perturbation growth in the vicinity of the storm in the 2-day forecast using the dry adjoint system of the Navy Operational Global Atmospheric Prediction System (NOGAPS, Hogan et al. 1991).

In recent years, NOGAPS has performed reasonably well in predicting tropical cyclone tracks (Peng et al. 2004), making it suitable for the present study. While moist physics play a key role in the development of tropical cyclones, our goal in the present study is to understand the role of the large-scale dry dynamics on TC evolution. As for the linear constraint, Reynolds and Rosmond (2003) have shown that synoptic-scale perturbation growth for mid-latitude systems can remain significantly linear out to three days.

*Corresponding author address: Melinda S. Peng, Code 7532, Marine Meteorology Division, Naval Research Laboratory, Monterey, CA 93943; e-mail: melinda.peng@nrlmey.navy.mil

2. Construction of Singular Vectors

The leading SV represents the fastest growing perturbation to a given trajectory in a linear sense. Consider a nonlinear model *M*, acting on a state vector $\mathbf{x}$, such that $M(\mathbf{x}_0) = \mathbf{x}_t$, where the subscript refers to the integration time. Let $\mathbf{x}_0'$ represent some perturbed initial state, such that $\mathbf{x}_0' - \mathbf{x}_0 = \mathbf{p}_0$ and $M(\mathbf{x}_0') - M(\mathbf{x}_0) = \mathbf{p}_t$. For linear perturbation growth, the initial perturbation can be propagated forward in time using the tangent forward propagator, **L**, representing the model equations of *M* linearized about the nonlinear trajectory, such that

$$\mathbf{L}\mathbf{p}_0 \cong \mathbf{p}_t . \quad (1)$$

L can be represented by its singular values and initial and final-time SVs as such:

$$\mathbf{L} = \mathbf{E}^{-1/2}\mathbf{U}\mathbf{D}\mathbf{V}^{\mathbf{T}}\mathbf{E}^{\mathbf{1}/2} \quad (2)$$

where **V** (**U**) are matrices with columns composed of the initial (final) SVs, and **D** is a diagonal matrix whose elements are the singular values of **L**. The superscript T denotes the transpose (thus $\mathbf{L}^{\mathbf{T}}$ is the adjoint of **L)**. **E** is the metric that defines how the perturbations are measured. Thus the SVs form an **E**-orthonormal set of vectors at initial and final time. The SVs satisfy the eigenvector equation $\mathbf{L}^{\mathbf{T}}\mathbf{E}\mathbf{L}\mathbf{y}_n = d_n^2\mathbf{E}\mathbf{y}_n$ where $\mathbf{y}_n = \mathbf{E}^{-1/2}\mathbf{v}_n$, and d_n and $\mathbf{v}_n$ are the n^{th} singular value and initial-time SV, respectively. The leading SV maximizes the ratio of the final perturbation energy to the initial perturbation energy:

$$\frac{\langle \mathbf{L}\mathbf{p}_0 ; \mathbf{E}\mathbf{L}\mathbf{p}_0 \rangle}{\langle \mathbf{p}_0 ; \mathbf{E}\mathbf{p}_0 \rangle} . \quad (3)$$

where < > represents a Euclidean inner product. The 2nd SV maximizes this ratio under the constraint of being orthogonal to the first SV, the 3rd SV maximizes this ratio under the constraint of being orthogonal to the first two SVs, and so on.

The SVs are calculated using the tangent and adjoint models of NOGAPS with a total energy metric at both initial and final time (Rosmond 1997). The SVs are calculated at a reduced resolution of T79L30, although the linearization is based on the trajectory from the full physics, high-resolution (T239 in the horizontal plane and 30 levels in the vertical) operational NOGAPS forecast. We apply this SV sensitivity to 2-day forecasts of northern hemisphere tropical cyclones between July and October 2003. Excluding some weak and short-lived storms, we choose 85 individual cases for 15 named TCs during that time period. A local projection operator (Buizza 1994) is employed to optimize final-time perturbation energy in a 20 x 20 degree box centered on the final-time storm position. As there are no other major weather systems within the optimization domain, the SVs at final time correspond to the final state of that storm. The initial SVs indicate regions where the 48-hour storm forecasts are most sensitive to changes in the analyses. The SV sensitivity pattern, **s**, is a composite of the vertically integrated total energy of the leading SVs, weighted by the singular values. The analysis fields from NOGAPS at one-degree resolution will be used for diagnostics and computation of PV and PV gradients.

3. Composite study

To a first order approximation, tropical cyclones either track westward to terminate over land within the tropics, or move poleward (recurve) into the middle latitudes and die over land or open oceans (Elsberry 1987). Based on this, we divide the 85 cases into two groups. The first group contains straight-moving cyclones and the second group contains recurving cyclones and irregular motion cyclones, referred to as the non-straight-moving group. Our hypothesis is that the initial SV sensitivity for different types of storm motion may exhibit different characteristics, in part due to the different characteristics of their environment. There are 30 cases in the straight-moving group (group one) and 55 cases in the non-straight-moving group (group two).

The distributions of the initial locations of the cyclones for the two groups are displayed in Fig. 1. Most of the cases in the straight-moving group are located between 10 and 20N, while most of the non-straight-moving storms are clustered at higher latitudes between 20 to 30N. The general environment characteristics for the two groups, illustrated through the average 500-hPa geopotential height for the two groups (Fig. 2), exhibit distinct differences. The straight-moving group is characterized by strong subtropical highs over the western Pacific and the Atlantic. The subtropical highs for the non-straight-moving groups are weaker and the mid-latitude synoptic waves are stronger than those in the non-straight-moving group. This is consistent with the climatology of Harr and Elsberry (1995a, b) and conforms with the understanding that straight-moving storm are associated with strong subtropical ridges while non-straight-moving (mostly recurving ones) storms are associated with the peripheral flow around weaker subtropical highs.

The composites of the SVs for these two groups are now compared. Composites are made of the SV sensitivities in a 60 by 60 degree longitude/latitude area centered on the position of the storm at the initial time. For the final time SVs, the composite are centered on the final position of the storms. Before the composites are made, all the SV sensitivity patterns are rotated such that the storm motions are pointing north in the diagrams.

a) Initial Singular Vectors

The composites of the initial SVs for the straight-moving group and the non-straight-moving group are depicted in Fig. 3. A common feature is that the maximum sensitivity is located within an annulus roughly 500 km from the storm center. For the straight-moving group, the most sensitive region lies in the rear right quadrant. The maximum for the non-straight-moving group is more evenly distributed within the annulus. For the straight-moving group, most of the individual maxima are concentrated near the composite maximum while the individual maxima in the non-straight-moving group exhibit more scatter around the annulus. Examination of individual fields at different levels indicates that, near the storm center the initial-time

SV sensitivity is dominated by the rotational kinetic energy component in the mid-lower troposphere. In the non-straight-moving group there are often additional local maxima in regions remote from the storm, and the initial-time SV sensitivity is usually dominated by potential energy in these regions.

Two major characteristics of these composites are explored in more detail. The first one is that the initial SV maximum is located at a considerable distance from the storm center (approximately 500 km). Through an examination of the analyzed variables and derived fields, we find that this initial SV maximum is located where the radial gradient of the vortex PV first changes sign. Fig. 4 shows the composite SVs and the composite radial PV gradient on the 320K isentropic surface for both groups. The potential vorticity is largest at the center of the tropical cyclone and decreases away from it until it reaches a local minimum where the vorticity (and potential vorticity) gradient changes sign, approximately 500 km from the center. Examination of individual cases indicates that this is true on a case-by-case basis, as well as in the composite average. The collocation of the SV maximum with the place where the PV gradient changes sign can be more clearly shown by the east-west cross section of the PV through the composite center on different isentropic surfaces (Fig. 4c and d). Throughout most of the troposphere, the PV gradient first changes sign at approximately the same location.

The second characteristic of the SV is the location of its maximum in the azimuthal direction. While the SV maxima are concentrated in the right rear quadrant of the storm in the straight-moving group, they are scattered around the cyclone in the non-straight-moving group. Examination of the wind fields in the individual cases indicates that the SV maximum is usually located in regions where the wind flow is toward the storm. For easier comparison, we decompose the total wind field into radial and tangential components on polar coordinates centered on the storm. The azimuthal wind is dominated by the rotation of the storm, while the radial component represents the flow moving toward (negative) or away (positive) from the storm. The collocation of the maximum SV and the flow toward the storm is stronger at lower levels for SV maxima located close to the storm, and at upper levels for SV maxima far away from the storm. The comparison of the composite of the SV and the composite of the radial wind speed for both groups shows that the SV maximum is located in the inward flow region (not shown).

To illustrate this relation individually, we plot the 850-hPa radial wind, with respect to the center of the storm, at the location of the SV maximum, for all cases except five cases associated with two coexisting storms (Fig. 5). The SV maxima are collocated with flow moving toward the storm for more than 75% of the cases. This relationship between the SV sensitivity and the radial inward flow indicates that the steering flow has a critical impact on the evolution of the storm. In the straight-moving group, the inward flow corresponding to the most sensitive region usually comes from the rear right quadrant of the storm. In the non-straight-moving group, the inward flow corresponding to the most sensitive region can be located in any direction, depending on the environmental influences.

As discussed previously, the maximum of the composite for the straight-moving group is located in the rear-right quadrant. This is also collocated with the composite inward flow toward the center. This inward flow appears to be associated with the steering flow of the cyclones, as explained next.

Early studies (Chan and Gray 1982) indicated that there is an angle between the TC motion and the steering flow in that cyclones typically move 15 degree to the left of the basic current (in the Northern Hemisphere). Meanwhile, model studies in idealized environments produce a deflection to the right of the basic current due to the beta effect (Anthes and Hoke 1975). This dichotomy has been explored by Holland (1983) showing different deflecting angles in different situations. Chan and Williams (1987) and Fiorino and Elsberry (1989) explained the beta-effect of a north by northwest gyre on TC motion through nonlinear vorticity advection. To support our hypothesis that the maximum SV is associated with the flow toward the storm center (representing the steering flow) and to explain the deflecting angle between the SV maximum and the storm motion, we composite the TC motion vector and the steering vector for group one (the straight-moving storms). The latter was computed with the 500 mb mean wind between 5 and 7 degrees distant from the storm center. The composite does show a right deflection of the TC motion from the steering flow, even though the angle between them is small. The importance of the

right rear quadrant with respect to the motion shown in group one is due to the fact that most of straight-moving storms are moving westward.

b) Final Singular Vectors

The final SVs represent the magnitude and distribution of the energy associated with the fastest growing perturbations at final time (the 2-day forecasts, in these cases). The composites of the final SVs for the two groups are depicted in Fig. 6. The composites are centered on the final storm position predicted by the full nonlinear high-resolution version of the model, and all the SVs are rotated so that the moving direction of the storm is to the north in the figure, as in the composites of the initial SVs. The finding that the maximum amplitude of the final SV sensitivity is clustered rather closely to the storm center indicates that the fast growing perturbations are primarily associated with the tropical cyclone of interest. Occasionally there is a smaller signal associated with other systems, (for example, the crescent-shaped signal in the front left quadrant of Fig. 6b). The broader pattern for the non-straight-moving group than for the straight-moving group also reflects the occasional influence of the SVs on other synoptic features in the vicinity of the TC.

The composite maximum is located roughly 200 km away from the storm center, collocated with the maximum of the radial PV gradient (Fig. 7). (Note that the composite in Figure 7 is made without rotating the SVs to be aligned with the storm movement, in contrast to Fig. 6). This is in contrast to the location of the initial SV maxima, which are located at the radial distance where the potential vorticity gradient changes sign. In a study of mid-latitude disturbances using SV diagnostics, Palmer et al. (1998), discuss how Rossby waves can propagate from weak PV gradient regions to strong PV gradient regions. The maxima in the initial and final SVs relative to the PV gradient distribution suggest that similar mechanism may be important in tropical cyclone evolution.

6. Summary

Singular vector (SV) sensitivity, calculated using the adjoint model of the U S. Navy Operation Global Atmosphere Prediction System, is used to study the dynamics associated with tropical cyclone evolution for the 2003 Northern Hemisphere summer season. For each model-predicted tropical cyclone, SVs are constructed that optimize perturbation energy within a 20 by 20 degree latitude/longitude box centered on the 48 hour forecast position of the cyclone. A total of 85 cases are examined excluding very weak and short-lived storms. The cased are grouped into straight-moving group and non-straight-moving group each containing 30 and 55 cases, respectively.

The initial SVs indicate regions where the 2-day forecast of the storm is most sensitive to changes in the analysis. Composites of the SVs for straight-moving cyclones and non-straight-moving cyclones that occurred in 2003 are examined. For both groups, the initial-time SV sensitivity exhibits a maximum within an annulus approximately 500 km from the center of the storms, in the region where the potential vorticity gradient of the vortex first changes sign. In the azimuthal direction, the composite initial-time SV maximum for the straight-moving group is located in the rear right quadrant with respect to the storm motion. The composite based on the non-straight-moving cyclones does not have a preferred quadrant in the vicinity of the storms and has larger amplitude away from the cyclones compared with the straight-moving storms, indicating more environmental influence on these storms. For both groups, the maximum initial sensitive areas are collocated with regions of flow moving toward the storm.

In summary, our results indicate that tropical cyclone forecasts are most sensitive to changes in the analysis where the radial potential vorticity gradient changes sign, and result in final-time maxima in regions where the potential vorticity gradient is sharpest. The results also highlight the importance of the flow moving toward the storm on subsequent storm evolution, and how non-straight-moving storms are more sensitive than straight-moving storms to changes in the analysis in remote regions. The relationship between the SV sensitivity and the potential vorticity suggests that shear instability (Fjørtorf 1951) and Rossby wave

propagation (Palmer et al. 1998; Moller and Montgomery 1999) may play important roles in the evolution of tropical cyclones.

Acknowledgement: This research is sponsored by the Naval Research Laboratory and the Office of Naval Research under program element 0601153N, project number BE-033-03-4M.

REFERENCES

Andrews, D. G., J. R. Holton, and C. B. Leovy, 1987: Middle atmosphere Dynamics. Academic Press. 489pp.

Anthes, R. A., and J. E. Hoke, 1975: Effect of horizontal divergence and latitude variation of Coriolis parameter on drift of a model hurricane. Mon. Rea. Rev., 103, 575-763.

Buizza, R., 1994: Localization of optimal perturbations using a projection operator. *Q. J. R. Meteorol. Soc.*, **120**, 1647-1681.

Chan, J.C.L., and W. M. Gray: Tropical cyclone movement and surrounding flow relationships. *Mon. Wea. Rev*., 110, 1354-1374.

----------, and R. T. Williams, 1987: Analytical and numerical studies of the beta-effect in tropical cyclone motion. Part I: Zero mean flow. *J. Atmos. Sci*., **44**, 1257-1265.

----------, Ko F.M.F., and Y.M. Lei, 2002: Relationship between potential vorticity tendency and tropical cyclone motion. *J. Atmos. Sci*., **59**, 1317-1336.

Elsberry, R. L., 1987: A global view of tropical cyclones. Office of Naval Research. International Workshop on Tropical Cyclones, Bangkok, Tailand, Nov. 25-Dec. 5, 1985. 185pp. (Editor)

Fiorino, M., and R. L. Elsberry, 1989: Some aspects of vortex structure related to tropical cyclone motion. *J. Atmos. Sci*., **46**, 975-990.

Fjørtorf, R., 1951: Stability properties of large-scale atmospheric disturbances. Pp. 454-463 in Compendium of Meteorology. American Meteorological Society, Boston, USA.

George, J. E., and W. M. Gray, 1976: Tropical cyclone motion and the surrounding parameter relationship. *J. Appl. Meteor*., 15, 1252-1264.

Harr, P. A., and R. L. Elsberry, 1995: Large-scale circulation variability over the tropical western North Pacific. Part I: Spatial patterns and tropical cyclone characteristics. *Mon. Wea. Rev*., 123, 1225-1244.

Hogan, T.F., and T.E. Rosmond, 1991: The description of the Navy Operational Global Atmospheric Prediction System's Spectral Forecast Model. *Mon. Wea. Rev*., **119**, 1786-1815.

Holland, G. J., 1983: Tropical cyclone motion: Environmental interaction plus a beta effect. *J. Atmos. Sci*., **40**, 328-342.

Majumdar, S.J., S. D. Aberson, C. H. Bishop, R. Buizza, M. S. Peng, and C.A. Reynolds, 2006: A comparison of adaptive observing guidance for Atlantic tropical cyclones. *Mon. Wea. Rev*. (in press).

Moller, J. D. and M. T. Montgomery, 1999: Vortex Rossby waves and hurricane intensification in a barotropic model. *J. Atmos. Sci.* **56**, 1674-1687.

Palmer, T. N., R. Gelaro, J. Barkmeijer, and R. Buizza, 1998: SVs, metrics and adaptive observations. *J. Atmos. Sci*., **55**, 633-653.

Peng, M. S., J. A. Ridout, and T. F. Hogan, 2004: Recent modifications of the Emanuel convective scheme in the Naval Operational Global Atmospheric Prediction System. *Mon. Wea. Rev.*, **132**, 1254-1268.

Rayleigh, Lord, 1880: On the stability or instability, of certain fluid motions. *Proc. London Math Soc*., **9**, 57-70.

Reynolds, C. A., R. Gelaro, and T. Rosmond, 2001: Relationship between singular vectors and transient features in the background flow. *Q. J. R. Meteorol. Soc.*, **127**, 1731-1760.

Reynolds, C.A. and T.E. Rosmond, 2003: Nonlinear growth of singular-vector-based perturbations. *Q. J. R. Meteorol. Soc*., **129**, 3059-3078.

Rosmond, T. E., 1997: A technical description of the NRL adjoint modeling system. NRL/MR/7532/97/7230. 53pp.

Shapiro, L. J., 1992: Hurricane vortex motion and evolution in a three-layer model. *J. Atmos. Sci*., **49**, 140-154.

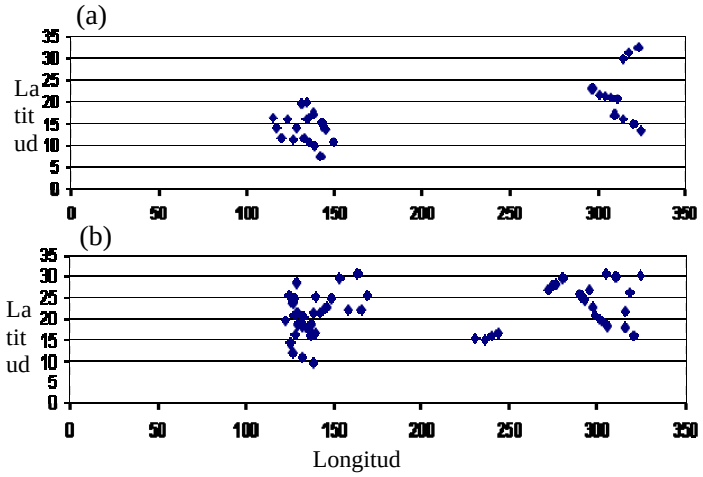

Figure 1. Geographical distributions of the initial positions of the TCs for: a) the straight-moving group, and b) the non-straight-moving group.

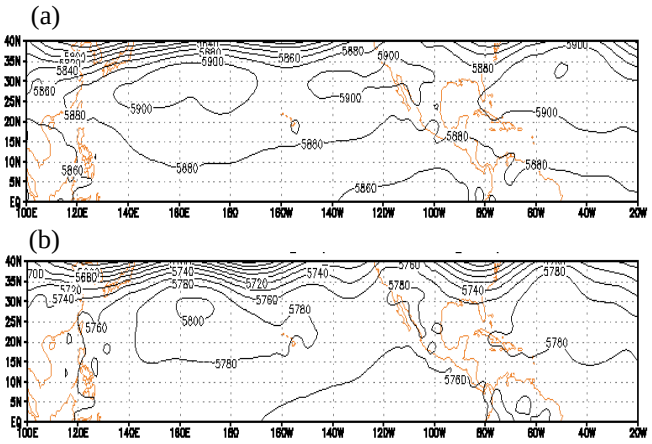

Figure 2. Mean of the 500-hPa geopotential height for: a) the straight-moving group, and b) the non-straight-moving group.

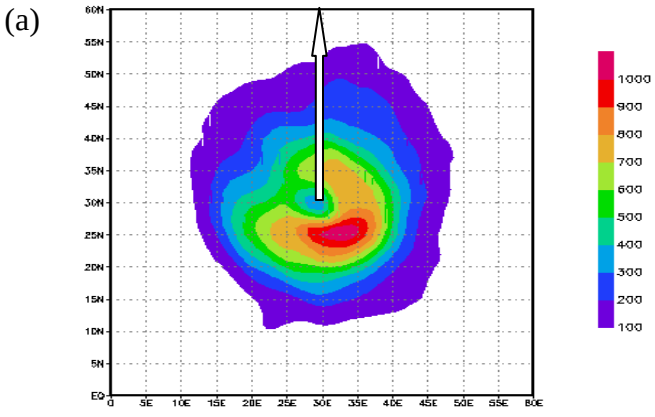

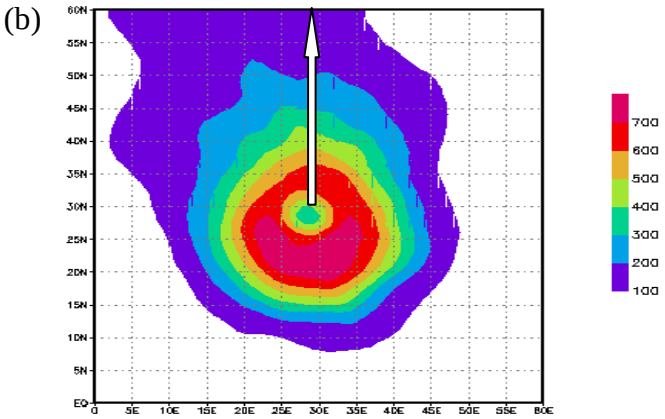

Figure 3. Composite of the SVs at the initial time for: a) straight-moving TCs, and b) recurving/erratic TCs. The units for the SVs are Jkg^{-1}, as in all the SV figures. All cyclone centers are at the center of the domain and the SVs are oriented such that the storm motion is northward, as indicated by the arrow.

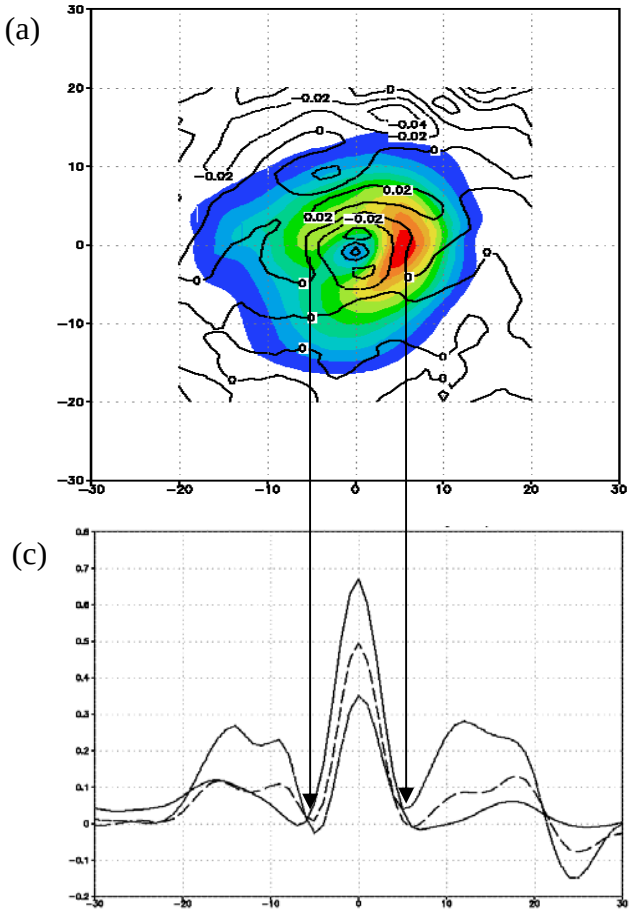

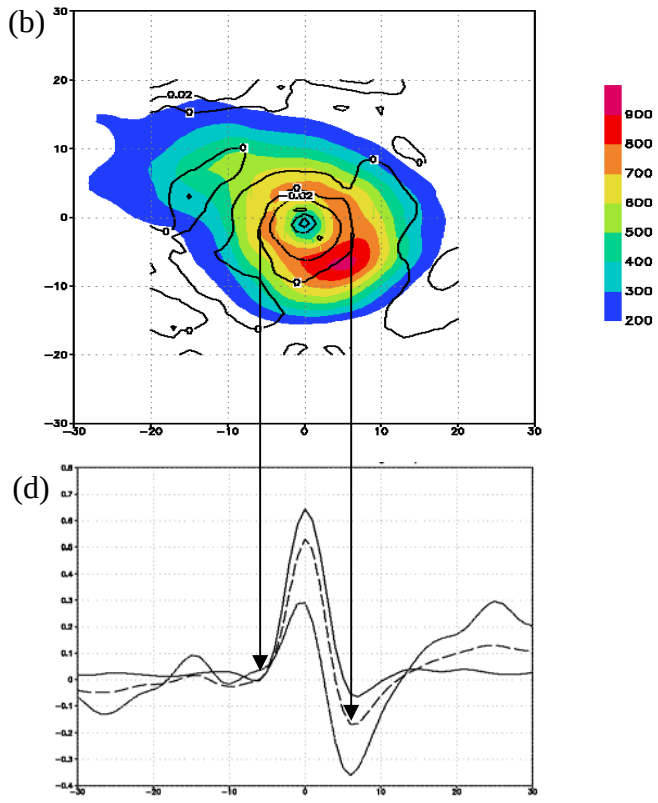

Figure 4. Composite of the SVs (shaded) at the initial time, as in Fig. 3, except that the fields are not rotated, and the potential vorticity gradient (on the 320 K surface) in the radial direction (contoured, 0.25×10^{-11}mKs^{-1}kg^{-1}) for: a) the straight-moving TCs; b) the non-straight moving TCs. Panels a) and b) share the same shading bar. Cross section of the potential vorticity (10^{-6}m^{2}Ks^{-1}kg^{-1}) across the storm center on the 320K surface (solid), 340K surface (dashed) and 350 K (dotted) for c) the straight-moving group and d) the non-straight moving group.

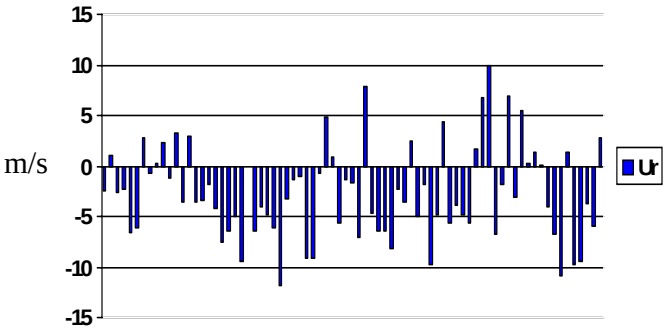

Figure 5. Wind speeds in the radial direction at the location of initial SV maximum on the 850-hPa surface for all cases except five cases associated with two coexisting storms in the western Pacific. Each bar represents the value for one case. Negative values indicate inward flow. See text for explanation of the vertical arrows.

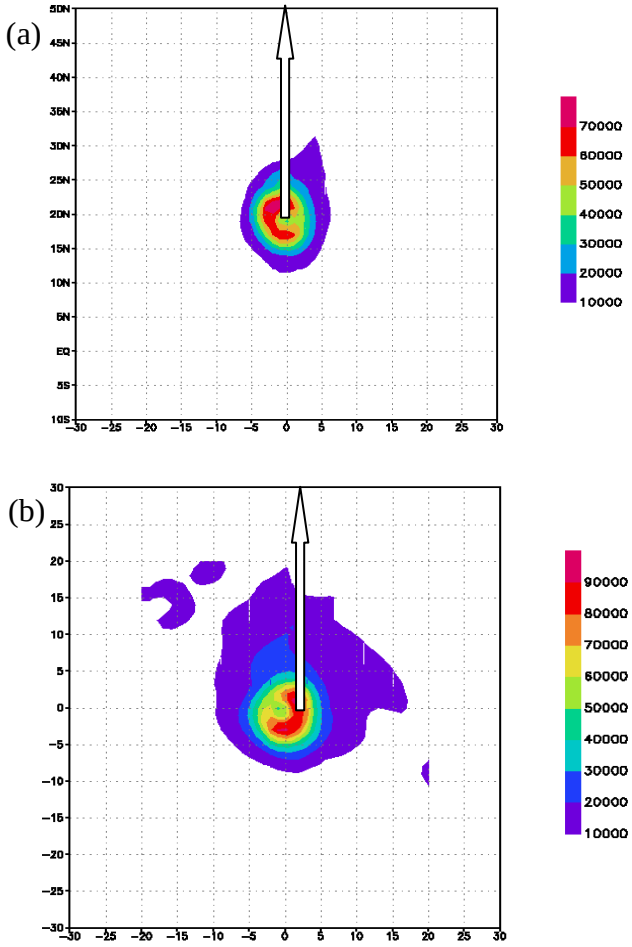

Figure 6. Composites of the final SVs for: a) the straight-moving group and b) the non-straight-moving group. All patterns are rotated first before the composite is made, with the TC movement pointing to the north (open arrows).

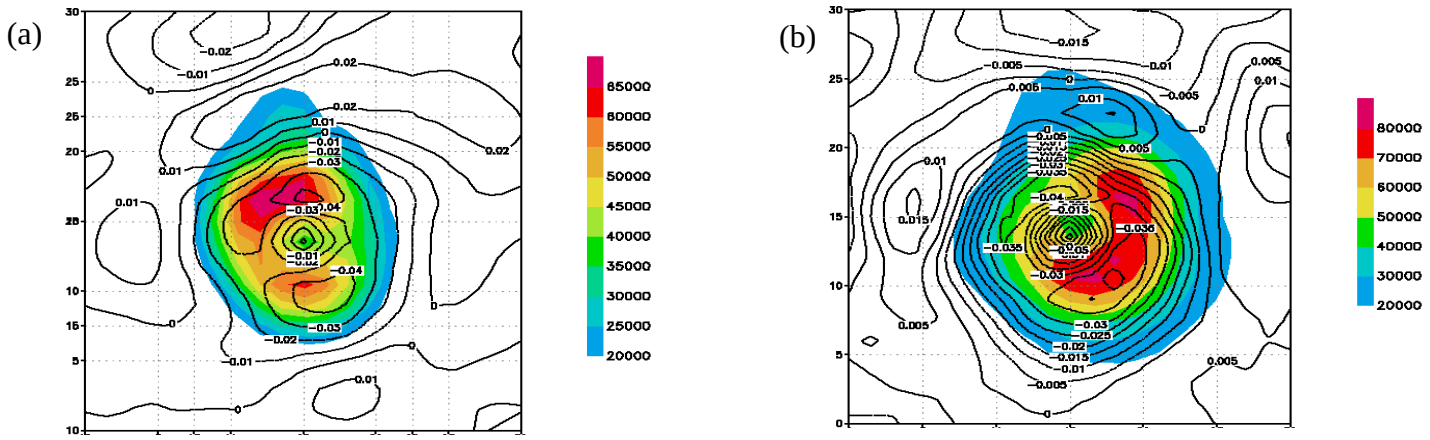

Figure 7. Composites of the final SVs (shaded), not rotated, along with the potential vorticity on the 330K surface (contours, 10^{-6}m^{2}Ks^{-1}kg^{-1}) for: a) the straight-moving group and b) the non-straight-moving group